Eur. Phys. J. B **53**, 29–34 (2006)
DOI: 10.1140/epjb/e2006-00339-x

THE EUROPEAN PHYSICAL JOURNAL B

Effect on alloying at the Fe/Ni(001) interfaces on the interlayer exchange coupling

A. Hadj-Larbi[1,a], A. Ziane[1], S. Bouarab[1], and C. Demangeat[2]

[1] Laboratoire de Physique et Chimie Quantique, Université Mouloud Mammeri de Tizi-Ouzou, 15000 Tizi-Ouzou, Algeria
[2] Institut de Physique et Chimie des Matériaux de Strasbourg, 23, rue du Loess, B.P. 43, 67034 Strasbourg Cedex 2, France

Received 25 April 2006 / Received in final form 4 August 2006
Published online 6 September 2006 –

Abstract. We investigate the stability of various ordered FeNi alloys at the interfaces of Fe/Ni superlattices by using ab initio density functional calculation. We consider an $Fe_{0.5}Ni_{0.5}$ ordered alloy of one or two monolayers thick at different positions beyond the interface and the possibility of an interdiffusion of a complete monolayer of Ni(Fe) in Fe(Ni) slab. An interfacial atomic layer of $Fe_{0.5}Ni_{0.5}$ exchanged with its adjacent Ni monolayers, leading to a buffer zone of Ni_3Fe composition is found to be the most stable structural configuration. For this atomic arrangement we investigate the magnetic profile and the resulting interlayer exchange coupling between the Ni slabs for Fe spacer thickness of 0 to 4 monolayers.

PACS. 75.70.Cn Magnetic properties of interfaces (multilayers, superlattices, heterostructures) – 73.21.Ac Multilayers – 75.50.Bb Fe and its alloys

1 Introduction

The Fe-Ni alloys can exist, in all compositions, in a chemically disordered form like a solid solution where the iron and nickel atoms occupy the crystal lattice sites randomly. The ordered phases are restricted to FeNi (tetrataenite) and $FeNi_3$ compositions and due to their low ordering temperatures they can be only synthesized by irradiation of disordered FeNi alloy with electron [1] or neutron [2] which accelerates diffusion. The ordered FeNi phase has also been found in meteorite specimens [1,3]. The diffusion in this condition is inaccessible in laboratory. From the magnetic point of view the Ni-Fe alloys are widely studied [4–7] because they present many anomalies with the composition. For example in the Invar alloy phase [7] containing 36% of Ni atoms, the Ni-Fe alloy exhibits extremely small thermal expansion coefficient, maximum lattice constant, and maximum magnetic moment. The deposition of Fe layers on the Ni substrate induces some ordered Ni-Fe alloying at the interfaces. Few papers about the types of Ni-Fe alloy that could form at the Ni-Fe interfaces in the Fe/Ni superlattices have appeared up to now in the literature [8–16]. Information about chemical and structural disorder at the Fe/Ni interfaces is lacking since low energy electron diffraction (LEED) measurements are not sensitive to the interface. However, many authors have detected interdiffusion between Ni and Fe at the interfaces. Ramchal et al. [8] have studied the spiral-like continuous spin-reorientation transition (SRT) of Fe/Ni bilayers on Cu(001). They explained the SRT which occurs around 2.5 Fe monolayers (MLs) by the existence of an intermixed interface consisting of an 50:50 FeNi alloy over 2 MLs. Fratucello et al. [9] have attributed the hyperfine field of about 28T at the Fe/Ni interface in the Ni/Fe/Ni(111) trilayer to the existence of an Fe-Ni fcc phase. Luches et al. [10] have found an intermixing depth of about 2.9 MLs for an epitaxial growth of ultrathin Fe films on Ni(001). Freeland et al. [11] investigated the fcc $Ni_{1-x}Fe_x$ thin films using a combination of Mössbauer spectroscopy and superconducting quantum interference device (SQUID) magnetometry. They obtained a continuous increase of the saturation magnetic moment (per atom) below $x \leq 0.65$ and a precipitous drop in moment at about $x = 0.65$. Lima et al. [4] have calculated the magnetic curve of $Ni_{1-x}Fe_x$ alloy by assuming a binomial distribution. The higher moment per atom was obtained in the fcc phase at $x = 0.5$. Hunter et al. [12] have used element-specific hysteresis measurements, based on X-ray magnetic circular dichroism (XMCD) technique and first principle calculations based on the non-collinear linear muffin-tin orbital method (LMTO) and plane wave pseudopotential, to investigate the magnetic $Ni_2Fe_2Ni_8$/Cu(001) trilayer. They obtained a small magnetic exchange interaction between the Fe and Ni layers which are directly in contact at the Fe/Ni interfaces, for lattice parameters close to 2.50 Å. The magnetic interaction at the interface is of antiferromagnetic and non-collinear type. They also obtain a decrease of the magnetic energy per atom for mixed

[a] e-mail: hadjlarbi@yahoo.com

Fe/Ni interfaces. Mavropoulos et al. [13] have studied with the Korringa, Kohn and Rostoker (KKR) Green-function method, the electronic structure of small Fe clusters having 1 to 9 atoms on Ni(001), Ni(111), Cu(001) and Cu(111) surfaces. They obtained a linear decrease of the Fe magnetic moment versus the number of Fe nearest neighbors. Martinez et al. [14] have studied the magnetism of Fe_9 nanocluster on Ni(001). The Ni-Fe interaction is ferromagnetic with a magnetic moment of $2.72-2.91\ \mu_B$ for the Fe atoms and $0.41-0.62\ \mu_B$ for the Ni atoms located at the surface and subsurface. Lounis et al. [15] have used the full potential KKR Green-function method to study Fe clusters (singles and dimers) on Ni(001) surface (adatoms) and embedded in Ni(001) (inatoms). They obtained a collinear FM coupling between Ni and Fe atoms. The magnetic moments of the Fe single adatoms and inatoms are $3.24\ \mu_B$, whereas for dimer adatoms and inatoms the moments are 3.10 and $2.88\ \mu_B$ respectively.

In a previous calculation [16] we had determined the magnetic profile and the interlayer exchange coupling (IEC) of $Fe_n/Ni_5(001)$ superlattices ($n = 1-5$) with abrupt and mixed interfaces made of a $Fe_{0.5}Ni_{0.5}$ ordered alloy of one ML thick. The main results obtained were: The magnetic coupling at the Fe-Ni interfaces is always of ferromagnetic (FM) type for both abrupt and alloyed interfaces. The Fe atoms in the $Fe_{0.5}Ni_{0.5}$ ML bear a relatively high magnetic moment ($\sim 2.6\ \mu_B$) as compared to the bulk (fcc) calculated value ($1.0\ \mu_B$ [16]). Alloying at the Ni/Fe interface leads always to lower energy and the IEC between Ni slabs through the Fe spacer in superlattices with mixed interfaces was found to be very different to that with perfect interfaces. We remind that IEC is defined as the total energy difference between the most stable magnetic arrangement of the Fe atoms for any interfacial atomic structure when two successive Ni slabs have their moments coupled parallel (P) and antiparallel (AP).

In the present paper we extend the investigation to some other ordered alloys that could form at the Ni/Fe interfaces. We first consider an $Fe_{0.5}Ni_{0.5}$ ordered alloy, one monolayer thick, at each Fe/Ni interface (Fig. 1b). Then we exchange this $Fe_{0.5}Ni_{0.5}$ layer at each interface with its adjacent Ni (Fig. 1c) or Fe layer (Fig. 1d). Secondly we exchange one Fe monolayer with one Ni monolayer at each Ni/Fe abrupt interface of the superlattice (Fig. 1e). Finally we consider an $Fe_{0.5}Ni_{0.5}$ ordered alloy, two monolayers thick, at each interface (Fig. 1f).

Let us remind that the atomic microstructure at the Ni-Fe interface is not experimentally well defined. Molecular dynamics simulations and possible relaxation effects at the interface is out of the scope of the method used in the present work. Nevertheless, the possible Ni-Fe compositional ordering considered here and their relative stability could give some insight on the interfacial interdiffusion.

The manuscript is organized as follows: in Section 2, we present the first principle method used in the calculation of the atomic magnetic moments, the total energy and the IEC. Section 3 is devoted to the results of the magnetic profiles and total energies of the different superlattices. A comparison of these energies leads to the ground state.

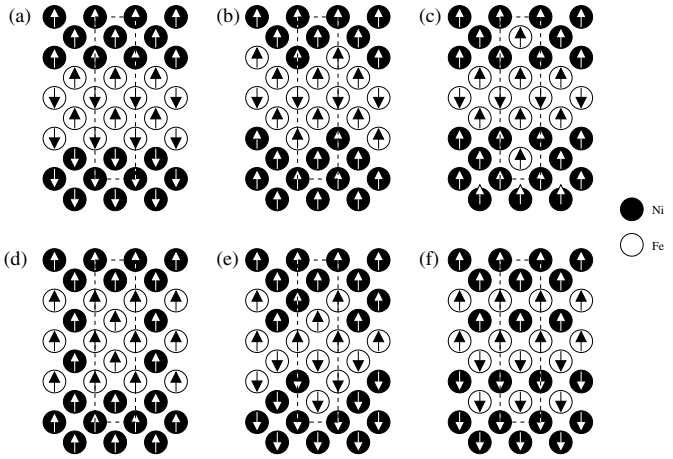

Fig. 1. The different ordered alloys considered at the Fe-Ni interfaces: (a) perfect interface; (b) $Fe_{0.5}Ni_{0.5}$ ML at interfaces; (c) $Fe_{0.5}Ni_{0.5}$ ML buried in the Ni layer; (d) $Fe_{0.5}Ni_{0.5}$ ML buried in the Fe layer; (e) two $Fe_{0.5}Ni_{0.5}$ MLs at Fe-Ni interface and one Fe ML interchanged with a Ni monolayer at each Ni/Fe interface (f). The unit cells considered in the calculations are delimited by dashed lines. For each superlattice only the most stable magnetic configuration is displayed.

We also discuss, in Section 3 the magnetic map of the ground state when the Fe spacer thickness is varied from 0 to 4 MLs. We conclude in Section 4 by the main points obtained in this work.

2 Theoretical model

Electronic structure calculations were performed using a scalar-relativistic version of the k-space tight-binding linear muffin-tin orbital (TB-LMTO) [17,18] in the atomic-sphere approximation (ASA). To fix the interatomic distances in the superlattices, the lattice parameters of the Ni and Fe fcc bulk were calculated through the minimization of the total energy [16]. Both Langreth-Mehl-Hu and Perdew-wang GGA functionals had been tested and finally the Langreth-Mehl-Hu functional was retained because it gives the best agreement for Fe with other calculations [19–26]. The ground state of bulk fcc Fe is antiferromagnetic (AF) with a lattice parameter of 6.56 au and a magnetic moment of $1.0\ \mu_B$. The ground state of bulk fcc Ni is ferromagnetic with a lattice parameter of 6.61 au and a magnetic moment of $0.63\ \mu_B$.

Figure 1 gives the six ordered alloys beyond the Fe/Ni interface considered in the present work. In order to determine the magnetic profile and the total energies of the Fe/Ni(001) superlattices with these various atomic arrangements at the interfaces we have used different supercells, (as delimited in Fig. 1) having the same number of atoms, (20 and 16 for Ni and Fe respectively), and two inequivalent atoms per plane.

To understand how these supercells are constructed one can simply start with a supercell composed of 4 Fe planes on 5 Ni planes (Fe_4/Ni_5), with 2 inequivalent atoms per plane. We double this supercell in order to

consider both parallel and antiparallel spin orientation of two successive Ni slabs [16]. This supercell corresponds to the superlattice with abrupt interfaces and is noted $(Fe_4/Ni_5)_2$. A schematic view of the abrupt Fe/Ni interface is displayed in Figure 1a. If an ordered $Fe_{0.5}Ni_{0.5}$ alloy, one ML thick is located at each Fe/Ni interface (Fig. 1b), the unit supercell is $(Ni_{0.5}Fe_{0.5}/Fe_3/Ni_{0.5}Fe_{0.5}/Ni_4)_2$. If the ordered $Fe_{0.5}Ni_{0.5}$ one ML thick is now exchanged with its adjacent Ni monolayer (Fig. 1c), the unit supercell is $(Ni_{0.5}Fe_{0.5}/Ni/Fe_3/Ni/Ni_{0.5}Fe_{0.5}/Ni_2)_2$ and if it is exchanged with its adjacent Fe ML (Fig. 1d), the unit supercell is $(Fe/Ni_{0.5}Fe_{0.5}/Fe/Ni_{0.5}Fe_{0.5}/Fe/Ni_4)_2$. The unit cell of chemical composition $(Ni_{0.5}Fe_{0.5})_2/Fe_2/(Ni_{0.5}Fe_{0.5})_2/Ni_3)_2$ corresponds to a superlattice with $Ni_{0.5}Fe_{0.5}$ ordered alloy, two MLs thick at each interface (Fig. 1e). If we exchange the Fe ML with its adjacent Ni ML at each Fe/Ni interface in the superlattice (Fig. 1f) with abrupt interfaces we obtain a unit supercell of composition $(Fe/Ni/Fe_2/Ni/Fe/Ni_3)_2$. The calculations are performed by using 72 irreducible k-points in the Brillouin zone.

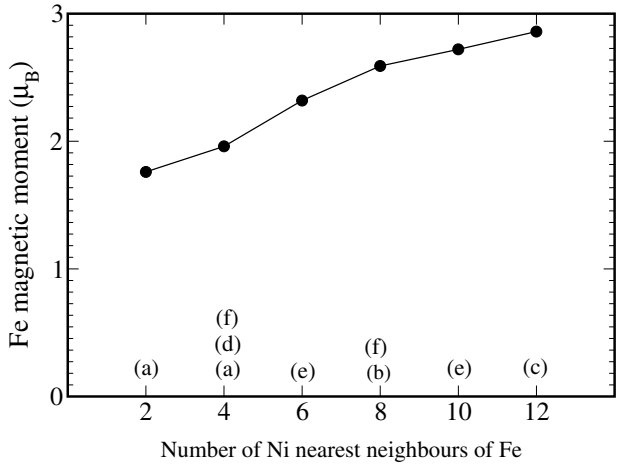

Fig. 2. The mean Fe magnetic moment as a function of the number of its Ni nearest neighbors. Each Fe atom with a given number of Ni neighbors can be present in several superlattices of Figure 1. The letters between brackets on the ordinate axis correspond to the superlattices displayed in Figure 1.

3 Magnetic map and total energy of the different structural arrangements at the Fe/Ni interfaces

The first part is devoted to the determination of the most stable magnetic arrangement of the Fe/Ni superlattices between the different chemical ordering at the interfaces displayed in Figure 1. Then we compare their total energies in order to deduce the FeNi ordered alloy which stabilizes the Fe/Ni superlattice. In the third part we focus on the magnetic profile and the corresponding IEC of this most stable atomic arrangement $(Ni_{0.5}Fe_{0.5}/Ni/Fe_n/Ni/Ni_{0.5}Fe_{0.5}/Ni_2)_2$ for an Fe spacer thickness varying from 0 to 4 MLs. For both IEC (P and AP), the electronic structure calculations are started from all possible spin configurations of the Fe atoms. We display in Figure 1 the different atomic arrangements considered at the interfaces together with the spin polarization on each atom. For each atomic arrangement we report only the most stable magnetic configuration. As we can see, the spin polarization in the Ni slab is of ferromagnetic type whereas it is of antiferromagnetic in the Fe spacer. Moreover in all cases considered, the coupling at the interfaces between the Fe and Ni layers as well as between $Fe_{0.5}Ni_{0.5}$ and Ni or Fe layers is always of ferromagnetic type (Fig. 1). The Fe-Ni ferromagnetic interaction at each interface enhances the magnetic moments of the Fe atoms as compared to bulk fcc state. These Fe moments increase with the number of Ni atoms in its first neighboring shell as displayed in Figure 2; this increase is almost linear with the number of its Ni nearest neighbors. On the other hand the presence of Ni atoms on the first coordination shell of Fe atoms screen the Fe-Fe antiferromagnetic coupling. We remind that the ground state of bulk fcc Fe is antiferromagnetic with a magnetic moment of 1.00 μ_B per atom [16]. The Fe atoms without any Ni nearest neighbor (Figs. 1a−1c) has a mean value of 1.02 μ_B, close to the bulk value. Besides, the Ni magnetic moments do not undergo significant variations as compared to the bulk Ni value (0.63 μ_B [16]). The values of the Ni moments vary between 0.59 and 0.67 μ_B.

The interlayer exchange coupling type, parallel or antiparallel, between successive Ni slabs shown in Figure 1 is linked to a competition between the ferromagnetic Ni-Fe interaction at the interfaces and the antiferromagnetic behavior of the Fe spacer. Thus the number of successive Fe MLs in the spacer affects strongly the IEC. For an odd number of Fe MLs, a parallel IEC (Figs. 1b−1d) is found to be the ground state. Otherwise the ground state corresponds to an antiparallel IEC.

The structural stability is determined by a comparison between the total energies per unit supercell of the superlattices reported in Figure 1. Each supercell unit has the same number of Ni atoms and the same number of Fe atoms. The interfacial atomic arrangement where an $Fe_{0.5}Ni_{0.5}$ ordered alloy of one monolayer thick exchanged with its adjacent Ni monolayer (Fig. 1c) is found to be the most stable. We report in Figure 3, the energy differences ΔE of the other atomic arrangements (Figs. 1a, 1b, 1d−1f) with the most stable one (Fig. 1c). From this figure, one can see that the Fe_4/Ni_5 superlattice with abrupt interface is the least stable. The formation of Ni-Fe alloy beyond the interface tends to stabilize the Fe/Ni superlattices in all cases. Our results can be explained according to the magnetic and structural properties of ordered NiFe compound [1–3,27–29]. Except for the superlattices of Figures 1a and 1b, we can consider the two MLs located between the Ni slab and the Fe spacer as a buffer. This buffer zone is a lattice with a $FeNi_3$ basis in the superlattice of Figure 1c which is the ground state. We know from literature that NiFe bulk alloy can exist at this composition. In Figure 1d the buffer is a lattice with Fe_3Ni as basis. It corresponds to the least stable state. For $Fe_{0.5}Ni_{0.5}$ ordered

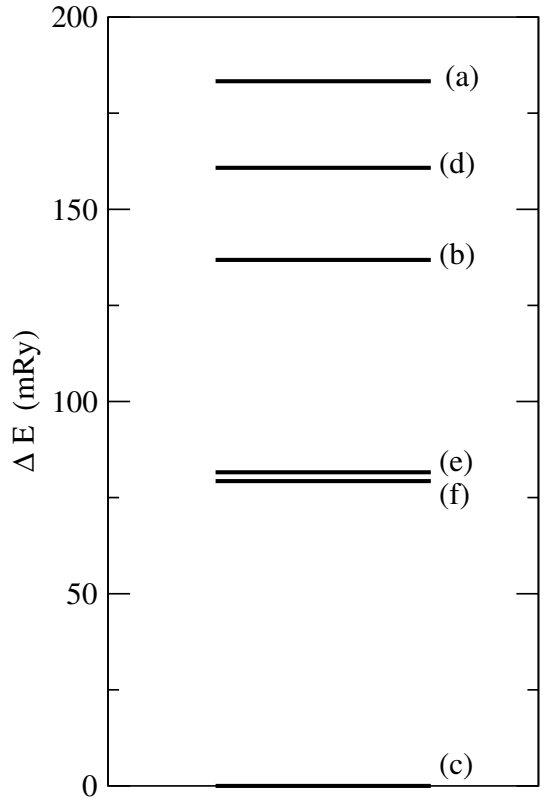

Fig. 3. The energy differences between the various metastable structural configurations (a, b, d, e, f of Fig. 1) and the ground state (Fig. 1c).

alloy, two MLs thick at each interface (Fig. 1e), the buffer has the same basis, FeNi, as the superlattice with Fe and Ni MLs interchanged at each abrupt interface (Fig. 1f). The energies of these two atomic structures are close. As mentioned in the introduction the ordered FeNi alloys with this composition can be produced by irradiation of disordered FeNi alloys [1–3].

After having determined the alloying at the Fe/Ni interfaces and the magnetic configuration which stabilizes the superlattice, (Fig. 1c), we investigate the magnetic profile and the resulting IEC of the corresponding superlattice of composition $Ni_{0.5}Fe_{0.5}/Ni/Fe_n/Ni/Ni_{0.5}Fe_{0.5}/Ni_2)_2$ when the Fe spacer thickness is varied from $n = 0$ to $n = 4$.

For $n = 1$ and 3 (odd number of Fe layers) the two $Ni_{0.5}Fe_{0.5}$ planes at both sides of the Fe spacer can be arranged symmetrically or asymmetrically. For $n = 1$ we report in Figure 4 these two types of atomic arrangements. In the symmetric arrangement (Fig. 4a), the Ni (Fe) atoms are invariant in a $2a$ translation in the (001) direction of the $Ni_{0.5}Fe_{0.5}$ ML through the Fe spacer, whereas in the asymmetric arrangement (Fig. 4b) the Ni and Fe atoms are only exchanged. The symmetric arrangement is energetically favored by 1.2 mRy and 0.25 mRy for $n = 1$ and $n = 3$ respectively. For $n = 0$, 2 and 4 (odd number of Fe layers), the two $Ni_{0.5}Fe_{0.5}$ planes at both sides of the Fe spacer are always symmetric. Figures 4c and 4d, give the atomic arrangement in the case of two Fe layers ($n = 2$).

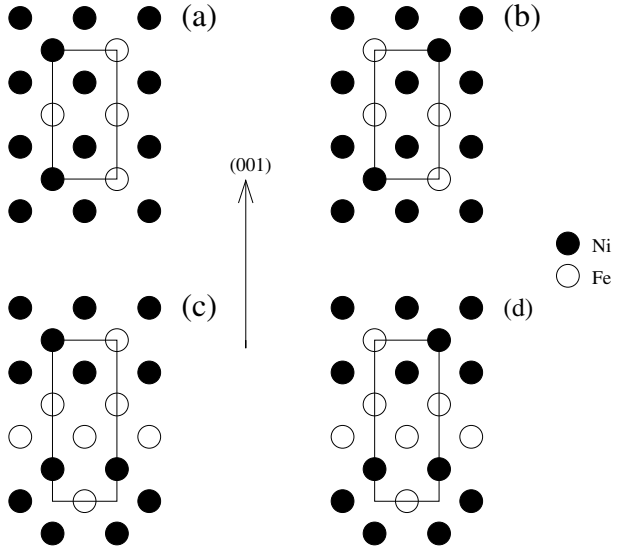

Fig. 4. Projection in the (001) direction of the different atomic arrangements considered beyond the Ni-Fe interface for $n = 1$ and $n = 2$. For $n = 1$ (odd number of iron layer), two arrangements are possible, a symmetric (a) and an asymmetric (b). For $n = 2$ (even number of Fe layers) the two arrangements (c) and (d) are symmetric.

The magnetic profile is displayed in Figure 5 for parallel and antiparallel alignment of the magnetic moments between two successive Ni slabs. For each Fe thickness and for both IEC type (AP or P), only the most stable configuration is reported. The buried Fe atom in the Ni film is surrounded by Ni atoms only on its first coordination shell (12 Ni atoms). These Ni atoms screen the antiferromagnetic interaction between the Fe neighbors so that the magnetic moment of the buried Fe atom is as high as 2.85 μ_B, independently of the Fe spacer thickness and of the IEC type. The Fe atoms in the Fe ML adjacent to the Ni plane have 8 and 4 nearest Ni neighbors for $n = 1$ and $n \geq 2$ respectively. When the Fe thickness is varied from $n = 1$ to $n = 2$ the magnetic moment of these atoms decreases from 2.58 to 2.34 μ_B for a parallel IEC and from 2.21 to 2.02 μ_B for an antiparallel IEC. For $n = 3$ and 4 these moments are close to 2.00 μ_B for parallel as well as for antiparallel IEC.

In the case of an antiparallel IEC, and for $n = 1, 3$, an in-plane antiferromagnetic configuration is obtained in the Fe central ML of the spacer. However this configuration is metastable as compared to the parallel IEC configuration. The layered antiferromagnetic behavior of the Fe spacer stabilizes the superlattice. We report in Figure 6 the calculated energy difference between the parallel and antiparallel IEC between two successive Ni slabs as function of the number (n) of Fe layers. The IEC presents an oscillatory behavior without a defined period.

The magnetic map and the IEC displayed in Figures 5 and 6 are qualitatively similar to those obtained in superlattice with $Fe_{0.5}Ni_{0.5}$, ordered alloy, one ML thick at the Fe/Ni interface (see Figs. 6 and 7 of Ref. [16]). This is not really surprising because both ordered alloyed

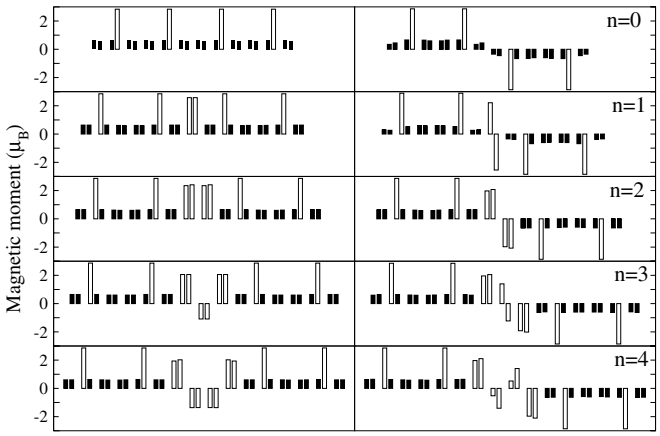

Fig. 5. Magnetic profiles (in μ_B) of $Fe_{0.5}Ni_{0.5}/Ni/Fe_n/Ni/Fe_{0.5}Ni_{0.5}/Ni_2$ ($n = 0, 1, 2, 3, 4$) superlattices. In the left and right panel the interlayer exchange couplings between Ni slabs are respectively of parallel and antiparallel type. Dark (open) bars represent the values of the magnetic moments on the Ni (Fe) atoms. Two magnetically inequivalent atoms per plane have been considered.

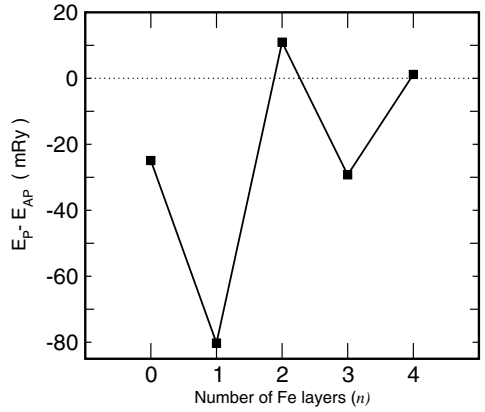

Fig. 6. The energy differences ($E_P - E_{AP}$) vs. the number of Fe monolayers (Fe_n is the spacer) in the $Fe_{0.5}Ni_{0.5}/Ni/Fe_n/Ni/Fe_{0.5}Ni_{0.5}/Ni_2$ superlattice ($n = 0, 1, 2, 3, 4$). E_P and E_{AP} correspond to a P and AP interlayer exchange coupling between two successive Ni slabs through the Fe spacer.

superlattices present similar chemical composition the only difference being in the position of the ordered monolayer. Thus the magnetic maps of the Fe spacer present striking similarities. Also the interlayer exchange couplings show a very similar qualitative behaviour in both cases although the present configuration being stable (Fig. 5) as compared to the metastable one reported in reference [16]. However, the IEC obtained with the two types of mixed interfaces are very different to those of superlattices with abrupt Fe/Ni interface (see Figs. 3 and 4 of Ref. [16]).

As it was stated above, the LMTO-ASA method used in our calculations does no allow atomic relaxation. However, to have an idea of the variation of the moments induced by the relaxation, we fixed the Ni-Fe distances to that of an fcc chemically ordered $FeNi_3$ which is found to stabilize the Ni-Fe interface. The moments do not change significantly (∼5%) and the energy differences between the various atomic configurations considered are quasi similar.

4 Conclusion

Two main points about the Fe/Ni superlattices are reported in this paper:

(i) The structural and the magnetic stability of the Fe/Ni superlattices with various mixing between iron and nickel atoms at the interfaces. All the systems considered present in common an Fe-Ni ferromagnetic coupling at the interfaces. The magnetic moment of the Fe atom increases quasi-linearly with the number of Ni atoms in its first coordination shell. The Fe/Ni superlattice is most stable if a buffer zone of two ordered monolayers thick, with $FeNi_3$ basis, is located between the Ni slab and the Fe spacer. It corresponds to the most stable state. However the ground state is not clearly identified. Some other complex interfacial microstructures not necessarily ordered could exist with lower energies but with a Fe:Ni composition close to 1:3.

(ii) The magnetic map and the interlayer exchange coupling of the ground state when the Fe spacer thickness varies between 0 and 4 MLs. The IEC between the Ni slabs through the Fe spacer oscillates as a function of the number of Fe MLs in the spacer but without specific behavior. It results from the Ni-Fe ferromagnetic coupling at the interfaces and the antiferromagnetic behavior of the spacer. The Fe atoms buried in the Ni layer have a magnetic moment of about 2.86 μ_B independently of the Fe thickness and of the IEC type. The Fe atoms of the spacer adjacent to the $FeNi_3$ buffer have higher magnetic moments as compared to the bulk value and their values depend on the Fe thickness for $n = 1$ and 2 and the IEC type whereas this dependence disappears for $n = 3$ and 4. These results are similar to those obtained previously [16] in the Fe/Ni superlattice with $Fe_{0.5}Ni_{0.5}$ ordered alloy, one ML thick at each interface and differ drastically from the results obtained in superlattices with abrupt Fe/Ni interface.

A. Hadj-Larbi acknowledges a grant from the Algerian Ministry of Higher Education and Scientific Research.

References

1. K.B. Reuter, D.B. Williams, J.I. Goldstein, Metall. Trans. A **20**, 711 (1989)
2. A. Chamberod, J. Laugier, J.M. Penisson, J. Magn. Magn. Mater. **10**, 139 (1979)
3. C.W Yang, D.B Williams, J.I Goldstein, J. Phase Equilib. **17**, 522 (1996)
4. E. Lima Jr, V. Drago, J. Magn. Magn. Mater. **280**, 251 (2004)

5. Y.A. Abdu, H. Annersten, T. Ericsson, P. Nordblad, J. Magn. Magn. Mater. **280**, 243 (2004)
6. A.R. Wildes, N. Cowlam, J. Magn. Magn. Mater. **272−276**, 536 (2004)
7. M. Van Schilfgaarde, I.A. Abrikosov, B. Johansson, Nature **400**, 46 (1999)
8. R. Ramchal, A.K. Schmid, M. Farle, H. Poppa, Phys. Rev. B **69**, 214401 (2004)
9. G.B. Fratucello, P. Vavassori, J. Magn. Magn. Mater. **260**, 480 (2003)
10. P. Luches, G.C. Gazzadi, A. di Bona, L. Marassi, L. Pasquali, S. Valeri, S. Nannarone, Surf. Sci. **419**, 207 (1999)
11. J.W. Freeland, I.L. Grigorov, J.C. Walker, Phys. Rev. B **57**, 80 (1998)
12. J. Hunter Dunn, O. Karis, C. Andersson, D. Arvanitis, R. Carr, A. Abrikosov, B. Sanyal, L. Bergqvist, O. Eriksson, Phys. Rev. Lett. **94**, 217202 (2005)
13. P. Mavropoulos, S. Lounis, R. Zeller, S. Blügel, Appl. Phys. A **82**, 103 (2006)
14. E. Martinez, A. Vega, R. Robles, R.C. Longo, L.J. Gallego, Comp. Mat. Sci. **35**, 307 (2006)
15. S. Lounis, Ph. Mavropoulos, P.H. Dederichs, S. Blügel, Phys. Rev. B **72**, 224437 (2005)
16. A. Hadj-Larbi, S. Bouarab, C. Demangeat, Phys. Rev. B **66**, 144428 (2002)
17. O.K. Andersen, O. Jepsen, Phys. Rev. Lett. **53**, 2571 (1984)
18. O.K. Andersen, Z. Pawlowska, O. Jepsen, Phys. Rev. B **34**, 5253 (1986)
19. P.M. Marcus, V.L. Moruzzi, Phys. Rev. B **60**, 69 (1999)
20. C.S. Wang, B.M. Klein, H. Krakauer, Phys. Rev. Lett. **54**, 852 (1985)
21. V.L. Moruzzi, P.M. Marcus, J. Kübler, Phys. Rev. B **39**, 6957 (1989)
22. H.C. Herper, E. Hoffmann, P. Entel, Phys. Rev. B **60**, 3839 (1999)
23. L. Kleinman, Phys. Rev. B **59**, 3314 (1999)
24. E.G. Moroni, G. Kresse, J. Hafner, Phys. Rev. B **56**, 15629 (1997)
25. H.J.F. Jansen, S.S. Peng, Phys. Rev. B **37**, 689 (1988)
26. K. Knöpfle, L.M. Sandratskii, J. Kübler, Phys. Rev. B **62**, 564 (2000)
27. Y. Mishin, M.J. Mehl, D.A. Papaconstantopoulos, Acta Materialia **53**, 4029 (2005)
28. E. Lima Jr, V. Drago, P.F.P. Fichtner, P.H. Domingues, Solid State Commun. **128**, 345 (2003)
29. E. Lima Jr, V. Drago, Phys. Status Solidi A **187**, 119 (2001)